

COUPLED-MODE ANALYSIS OF LINE PARAMETERS OF COUPLED MICROSTRIP LINES

M. Matsunaga, M. Katayama and K. Yasumoto

Department of Computer Science and Communication Engineering
Kyushu University 36
Fukuoka 812-8581, Japan

- 1. Introduction**
 - 2. Formulation**
 - 2.1 Coupled-mode Equations
 - 2.2 Characteristic Mode Impedances
 - 3. Numerical Examples**
 - 4. Concluding Remarks**
 - 5. Acknowledgment**
- References**

1. INTRODUCTION

Multilayered and multiconductor transmission lines are widely used for many applications in the microwave and millimeter-wave integrated-circuit devices, such as filters, power dividers, and directional couplers. These circuits are usually designed by utilizing the knowledge of mode propagation constants, characteristic mode impedances, and ratios of modal line currents or modal line voltages for the coupled lines. When the operating frequency is relatively low, these line parameters may be obtained [1] in terms of the quasi-static capacitances and inductances of coupled TEM lines. However, as the frequency is increased, the electromagnetic nature in the coupled lines becomes important. This requires an evaluation of the line parameters using the full-wave analysis [2]. Although various numerical techniques [3] have been developed for the rigorous analysis of coupled lines, those direct solution methods become much more involved and are very time consuming

computationally when the number of lines increases.

In this paper, we shall present an approximate method to obtain the line parameters of coupled microstrip lines based on the full-wave analysis. The technique uses the coupled-mode equations [4, 5] which describe the wave propagation along the lines in terms of the coupled-differential equations for the amplitudes of currents in each line. The coupling matrix in the equations, expressed by overlap integrals between the eigenmode fields of each isolated single line, characterizes the electromagnetic properties of the coupled lines. The eigenvalues and eigenvectors of the matrix give the propagation constants and the ratios of currents on the lines for the coupled modes. The characteristic mode impedances for the total power and the partial power definitions [6, 7] are expressed in terms of those eigenvectors and current ratios. Then all of the line parameters are determined by the elements of coupling matrix in the coupled-mode equations.

The coupled-mode theory provides simpler analytical and numerical procedures than the direct numerical solution methods, and is easy to apply to configurations of multiple nonidentical coupled lines, since the eigenmode solutions of the isolated single line are readily obtained using the Galerkin's moment method in the spectral domain. To verify the proposed theory, two nonidentical coupled lines and three nonidentical coupled lines in a single plane, and two identical coupled lines in dual planes are chosen as models of the coupled-mode analysis. The numerical results for the mode propagation constants and characteristic mode impedances are compared with those [2, 7–10] obtained by the direct numerical solution method for the coupled-lines. It is shown that both results are in good agreement.

2. FORMULATION

2.1 Coupled-mode Equations

Consider coupled N microstrip lines situated in a M -layered dielectric substrate over a ground plane of perfect conductor. The strips of widths $2w_\nu$ ($\nu = 1, 2, \dots, N$) are assumed to be perfect conductors of zero thickness. The center of the ν -th strip is located at $x = x_\nu$. The thickness and relative dielectric constant of the i -th layer are h_i and ε_i ($i = 1, 2, \dots, M$), respectively. The coupled-mode equations for the coupled-microstrip lines are formulated using the generalized

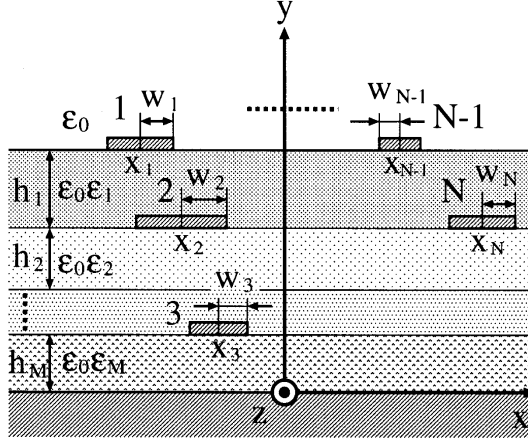


Figure 1. Cross section of multilayered multiple-coupled microstrip lines.

reciprocity relation [4, 5]. The electromagnetic fields and currents of the coupled lines in Fig. 1 are approximated as follows:

$$\mathbf{E}(x, y, z) = \sum_{\nu=1}^N a_{\nu}(z) \mathbf{e}_{\nu}(x, y) \quad (1)$$

$$\mathbf{H}(x, y, z) = \sum_{\nu=1}^N a_{\nu}(z) \mathbf{h}_{\nu}(x, y) \quad (2)$$

$$\mathbf{J}(x, y, z) = \sum_{\nu=1}^N a_{\nu}(z) \mathbf{j}_{\nu}(x, y) \quad (3)$$

where $a_{\nu}(z)$ are unknown amplitude functions and $\mathbf{e}_{\nu}(x, y)$, $\mathbf{h}_{\nu}(x, y)$ and $\mathbf{j}_{\nu}(x, y)$ are the eigenmode functions for the fields and currents propagating in the $+z$ direction along N each microstrip in isolation as shown in Fig. 2. The eigenmode fields and currents propagating in the $-z$ direction in the respective N isolated microstrips are expressed as follow:

$$\mathbf{E}'_{\nu} = [\mathbf{e}_{\nu,t}(x, y) - \hat{\mathbf{z}}e_{\nu,z}(x, y)] \exp(i\beta_{\nu}^{(0)}z) \quad (4)$$

$$\mathbf{H}'_{\nu} = [-\mathbf{h}_{\nu,t}(x, y) + \hat{\mathbf{z}}h_{\nu,z}(x, y)] \exp(i\beta_{\nu}^{(0)}z) \quad (5)$$

$$\mathbf{J}'_{\nu} = [\hat{\mathbf{x}}j_{\nu,x}(x, y) - \hat{\mathbf{z}}j_{\nu,z}(x, y)] \exp(i\beta_{\nu}^{(0)}z) \quad (6)$$

$(\nu = 1, 2, \dots, N)$

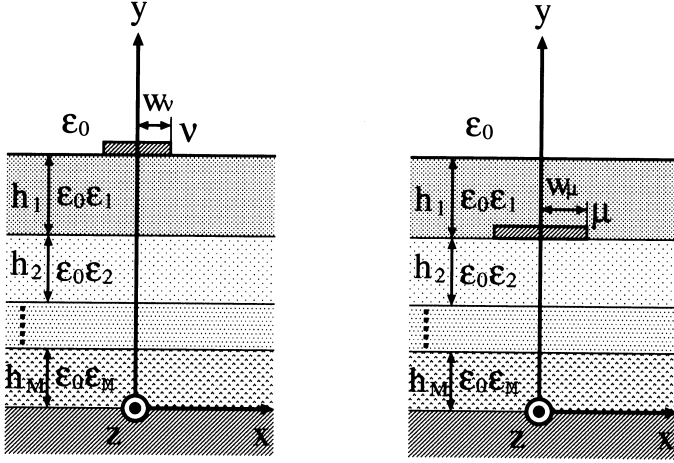


Figure 2. Isolated single microstrip " ν " and " μ " located in the original dielectric layers as shown in Fig. 1.

where $\beta_\nu^{(0)}$ is the propagation constant of the isolated ν -th microstrip, and the subscripts t , x , and z denote the transverse, x , and z components of the indicated vectors, respectively. Substituting Eqs. (1)–(3) and Eqs. (4)–(6) for each of N isolated single microstrips into the generalized reciprocity relation [4], the coupled-differential equations governing the evolutions of modal amplitudes $a_\nu(z)$ are derived as follows:

$$\frac{d}{dz}\mathbf{a} = -i[\mathbf{C}]\mathbf{a} \quad (7)$$

with

$$\mathbf{a} = [a_1(z) \ a_2(z) \ \dots \ a_N(z)]^T \quad (8)$$

$$[\mathbf{C}] = [\mathbf{M}]^{-1}[\mathbf{K}] \quad (9)$$

$$K_{\nu\mu} = \beta_\nu^{(0)} M_{\nu\mu} + Q_{\nu\mu} \quad (10)$$

$$M_{\nu\mu} = \frac{1}{2}(N_{\nu\mu} + N_{\mu\nu}) \quad (11)$$

$$N_{\nu\mu} = \frac{1}{2} \int_S [\mathbf{e}_\nu(x, y) \times \mathbf{h}_\mu(x, y)] \cdot \hat{\mathbf{z}} \, dx dy \quad (12)$$

$$Q_{\nu\mu} = -\frac{i}{4} \int_{l_\mu} [e_{\nu,x}(x, y) j_{\mu,x}(x, y) - e_{\nu,z}(x, y) j_{\mu,z}(x, y)] \, dx dy \quad (13)$$

$$(\nu, \mu = 1, 2, \dots, N)$$

where S represents the cross-sectional area of the structure, l_μ denotes the cross-sectional contour of the μ -th line, and the eigenmode fields and currents in the isolated lines are normalized so that $N_{\nu\nu} = 1$. Note that $Q_{\nu\nu} = 0$ since $e_{\nu,x}(x, y) = e_{\nu,z}(x, y) = 0$ on the surface of the ν -th line. Equation (7) is the coupled-mode equations which play the same role as the transmission line equations in the quasi-static approach [1]. The solutions determine the propagation constant β_m of the coupled mode m and the modal amplitude $a_{\nu m}$ of the current on the ν -th line.

The problem of coupled N microstrip lines was reduced to that of isolated N microstrip lines. When the eigenmode fields and currents for the isolated N lines are obtained, the coupling coefficients $K_{\nu\mu}$, $N_{\nu\mu}$, and $Q_{\nu\mu}$ governing the interaction between the ν -th and μ -th lines are easily calculated by the overlap integrals given by Eqs. (12) and (13). For the microstrips of zero thickness, these integrals can be efficiently performed [4, 5] in the spectral domain by using the Galerkin's moment method solutions for the conventional single microstrip. The details of this numerical method have been well documented in the open literature [3]. The reciprocity relation [4, 5] between the eigenmode fields of the isolated ν -th and μ -th lines leads to the identity

$$\beta_\nu^{(0)} M_{\nu\mu} + K_{\nu\mu} = \beta_\mu^{(0)} M_{\mu\nu} + K_{\mu\nu}. \quad (14)$$

This relation reduces the calculation of the coupling matrix $[\mathbf{C}]$ in Eq. (7).

2.2 Characteristic Mode Impedances

The normal mode parameters of the coupled microstrip lines are the mode propagation constants, the modal current ratios on the N lines, and the characteristic mode impedances of the N lines. The propagation constants are given by the eigenvalues of the coupling matrix $[\mathbf{C}]$ and the associated eigenvectors determine the modal current ratios. The characteristic mode impedances can be derived by utilizing these solutions to the coupled-mode equations (7). The current on the ν -th line for mode m is given by

$$I_{\nu m} = a_{\nu m} e^{-i\beta_m z} \int_{x_\nu - w_\nu}^{x_\nu + w_\nu} j_{\nu,z}(x) dx \quad (\nu, m = 1, 2, \dots, N) \quad (15)$$

where $j_{\nu,z}(x)$ is the z -component of current density on the isolated ν -th line, and $a_{\nu m}$ denotes the ν -th component of the m -th eigenvector of $[\mathbf{C}]$.

When the problem of the isolated ν -th microstrip is solved by Galerkin's moment method with Chebyshev polynomial basis functions, $I_{\nu m}$ is calculated as follows:

$$\begin{aligned} I_{\nu m} &= a_{\nu m} \int_{x_\nu - w_\nu}^{x_\nu + w_\nu} \sum_{n=0}^{N-1} \gamma_{\nu n} \frac{T_n\left(\frac{x - x_\nu}{w_\nu}\right)}{\sqrt{1 - \left(\frac{x - x_\nu}{w_\nu}\right)^2}} dx \\ &= a_{\nu m} w_\nu \int_{-1}^1 \frac{1}{\sqrt{1 - t^2}} \sum_{n=0}^{N-1} \gamma_{\nu n} T_n(t) dt \\ &= a_{\nu m} w_\nu \gamma_{\nu 0} \pi \end{aligned} \quad (16)$$

where $T_n(t)$ is a Chebyshev polynomial of order n of the first kind and $\gamma_{\nu n}$ is the expansion coefficient of the longitudinal current component $j_{\nu,z}(x)$. The characteristic mode impedance $Z_{c,\nu m}$ of the ν -th line for mode m is defined as

$$V_{\nu m} = Z_{c,\nu m} I_{\nu m} \quad (17)$$

where $V_{\nu m}$ represents the eigenvoltage. The eigencurrent $I_{\nu m}$ and eigenvoltage $V_{\nu m}$ are related to the power carried by mode m in the z direction. There are two different definitions [7] for the power. When the total power definition is used, we have

$$\frac{1}{2} \sum_{\nu=1}^N V_{\nu m} I_{\nu m}^* = P_m \delta_{mm'} \quad (18)$$

where P_m is the total power carried by mode m and $\delta_{mm'}$ is the Kronecker's delta. Using the solutions to Eq. (7), P_m is expressed as follows:

$$\begin{aligned} P_m &= \frac{1}{2} \int_S (\mathbf{E}_m \times \mathbf{H}_m^*) \cdot \hat{\mathbf{z}} dx dy \\ &= \sum_{\nu=1}^N \left(\sum_{\mu=1}^N a_{\nu m} a_{\mu m}^* N_{\nu \mu} \right) \end{aligned} \quad (19)$$

where \mathbf{E}_m and \mathbf{H}_m are the total electric and magnetic fields for mode m and $a_{\nu m}$ is real, because the structure is assumed to be lossless.

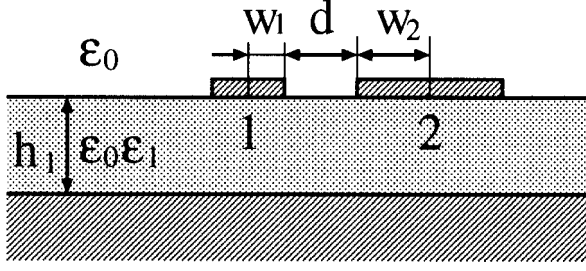


Figure 3. Cross section of two nonidentical coupled microstrip lines.

Equations (16), (17), and (19) are substituted into Eq. (18) to obtain the expression of $Z_{c,\nu m}$ in terms of the solutions to the coupled-mode equations (7). The results are illustrated for the coupled two microstrip lines shown in Fig. 3 as follows:

$$Z_{c,11} = \frac{2P_1}{(a_{11}w_1\gamma_{10})^2(1 - R_{21}^i/R_{22}^i)} \quad (20)$$

$$Z_{c,21} = \frac{2P_1}{(a_{21}w_2\gamma_{20})^2(1 - R_{22}^i/R_{21}^i)} \quad (21)$$

$$Z_{c,12} = \frac{2P_2}{(a_{12}w_1\gamma_{10})^2(1 - R_{22}^i/R_{21}^i)} \quad (22)$$

$$Z_{c,22} = \frac{2P_2}{(a_{22}w_2\gamma_{20})^2(1 - R_{21}^i/R_{22}^i)} \quad (23)$$

with

$$P_m = a_{1m}^2 + a_{2m}^2 + 2a_{1m}a_{2m}M_{12} \quad (m = 1, 2) \quad (24)$$

$$R_{21}^i = \frac{I_{21}}{I_{11}} = \frac{a_{21}w_2\gamma_{20}}{a_{11}w_1\gamma_{10}} \quad (25)$$

$$R_{22}^i = \frac{I_{22}}{I_{12}} = \frac{a_{22}w_2\gamma_{20}}{a_{12}w_1\gamma_{10}} \quad (26)$$

where $R_{\nu m}^i$ is the ratio of current amplitudes on the two lines for mode m . When the partial power $P_{\nu m}$ definition is employed, on the other hand, we have

$$\frac{1}{2}V_{\nu m}I_{\nu m}^* = P_{\nu m} \quad (27)$$

with

$$\begin{aligned}
 P_{\nu m} &= \frac{1}{2} \int_S (\mathbf{E}_m \times \mathbf{H}_{\nu m}^*) \cdot \hat{\mathbf{z}} \, dx dy \\
 &= \sum_{\mu=1}^N a_{\mu m} a_{\nu m} N_{\mu \nu}
 \end{aligned} \tag{28}$$

where $\mathbf{H}_{\nu m}$ represents the magnetic field for mode m produced by the current on the ν -th line. Using Eq. (17) in Eq. (27), the characteristic mode impedance $Z_{c,\nu m}$ based on the partial power definition is derived. For the coupled two microstrip lines shown in Fig. 3, they are obtained as follows:

$$Z_{c,11} = \frac{2P_{11}}{(a_{11}w_1\gamma_{10})^2} \tag{29}$$

$$Z_{c,21} = \frac{2P_{21}}{(a_{21}w_2\gamma_{20})^2} \tag{30}$$

$$Z_{c,12} = \frac{2P_{12}}{(a_{12}w_1\gamma_{10})^2} \tag{31}$$

$$Z_{c,22} = \frac{2P_{22}}{(a_{22}w_2\gamma_{20})^2} \tag{32}$$

where

$$P_{1m} = a_{1m}^2 + a_{2m}a_{1m}N_{21} \tag{33}$$

$$P_{2m} = a_{1m}a_{2m}N_{12} + a_{2m}^2. \tag{34}$$

The propagation constants β_m , current ratios $R_{\nu m}$, and characteristic mode impedances $Z_{c,\nu m}$ are used to derive the elements of the impedance matrix and scattering matrix for the $2N$ -port circuits for the coupled N microstrip lines. The results [11] are of the same form as those [1] obtained from the transmission-line equations in the quasi-static approach. The important difference is that the current ratios and modal characteristic impedances in the present approach are obtained in terms of the electromagnetic coupling coefficients, whereas those of the quasi-static approach are given in terms of the elements of the capacitance matrix.

3. NUMERICAL EXAMPLES

To validate the proposed theory, microstrip line structures as shown in Figs. 3, 5, and 8 are chosen as models for the coupled-mode analysis.

Figure 3 shows the cross section of coupled two microstrip lines in a single plane with $w_1 = 0.3$ mm, $w_2 = 0.6$ mm, $h_1 = 0.635$ mm, and $\epsilon_1 = 9.7$. The effective dielectric constants for the coupled modes 1 and 2 are plotted in Fig. 4 as functions of frequency for the separation distance $d = 0.4$ mm and compared with those [8] obtained by the direct numerical solution method. Both results are in good agreement. The modes 1 and 2 are usually referred to as c mode and π mode, respectively. In Table 1 a typical set of the characteristic mode impedances calculated at 10 GHz using Eqs. (20)–(23) and Eqs. (29)–(32) are compared with values of [9] for several separation distances. The coupled-mode theory yields nearly identical results for the two definitions of characteristic mode impedances and both results satisfy the relation $Z_{c,11}/Z_{c,21} = Z_{c,12}/Z_{c,22}$ given in [1] within the relative errors less than 10^{-4} . The discrepancies between the present results and the values of [9] are less than 8% except for $Z_{c,12}$ and $Z_{c,22}$ with $d = 0.1$ mm. It is noted that the relative errors of [9] for satisfying the relation $Z_{c,11}/Z_{c,21} = Z_{c,12}/Z_{c,22}$ are 10^{-2} to 10^{-3} .

The second example is coupled three microstrip lines in a single plane as shown in Fig. 5 where $w_1 = 0.15$ mm, $w_2 = 0.3$ mm, $w_3 = 0.6$ mm, $d_{12} = 0.2$ mm, $d_{23} = 0.4$ mm, $h_1 = 0.635$ mm, and $\epsilon_1 = 9.8$. Figure 6 shows the effective dielectric constants calculated for the coupled modes 1, 2, and 3 as functions of frequency. It is seen that the results are in very good agreement with those [10] obtained by the spectral domain method for the coupled three lines. The characteristic mode impedances $Z_{c,11}$ to $Z_{c,33}$ calculated using the total power definition are shown in Fig. 7 and compared with the values of [10]. A good agreement between both results is observed except for $Z_{c,11}$ in the high frequency region. The results of the coupled-mode analysis using the partial power definition are omitted, because they are nearly identical to those of the total power definition.

Finally we consider coupled two microstrip lines in dual planes as shown in Fig. 8 where $w_1 = w_2 = 5\mu\text{m}$, $h_1 = h_2 = 10\mu\text{m}$, and $\epsilon_1 = \epsilon_2 = 4.0$. The effective dielectric constants of the coupled-modes 1 and 2 calculated for $d = 30\mu\text{m}$ are shown in Fig. 9 and compared with those [2] obtained by the direct spectral domain method. It is seen that both results agree very well. Figure 10 shows the comparison of the characteristic mode impedances. The results of the coupled-mode analysis are in good agreement with those of [2] except for $Z_{c,11}$. The results of [2] have been obtained using the partial power definition and

(a) Total power definition (20)–(23)

d[mm]	$Z_{c,11}[\Omega]$	$Z_{c,21}[\Omega]$	$Z_{c,12}[\Omega]$	$Z_{c,22}[\Omega]$
0.1	70.98	41.29	40.81	23.74
0.2	66.26	40.11	43.16	26.13
0.3	63.11	39.18	44.86	27.85
0.4	60.85	38.45	46.13	29.15
0.5	59.18	37.87	47.10	30.14
0.6	57.91	37.41	47.85	30.91

(b) Partial power definition (29)–(32)

d[mm]	$Z_{c,11}[\Omega]$	$Z_{c,21}[\Omega]$	$Z_{c,12}[\Omega]$	$Z_{c,22}[\Omega]$
0.1	71.26	41.20	40.70	23.95
0.2	66.50	40.04	43.07	26.30
0.3	63.32	39.13	44.79	27.99
0.4	61.04	38.41	46.07	29.26
0.5	59.34	37.84	47.06	30.24
0.6	58.05	37.39	47.82	30.99

(c) Reference [9]

d[mm]	$Z_{c,11}[\Omega]$	$Z_{c,21}[\Omega]$	$Z_{c,12}[\Omega]$	$Z_{c,22}[\Omega]$
0.1	75.50	43.90	35.00	20.70
0.2	71.43	42.86	39.94	24.30
0.3	68.57	42.14	42.82	26.43
0.4	66.43	41.43	44.29	27.86
0.5	64.29	40.71	46.43	29.29
0.6	63.21	40.00	47.50	30.35

Table 1. Comparison of the characteristic mode impedances of two nonidentical coupled microstrip lines at $f = 10$ GHz. The values of other parameters are the same as those in Fig. 4.

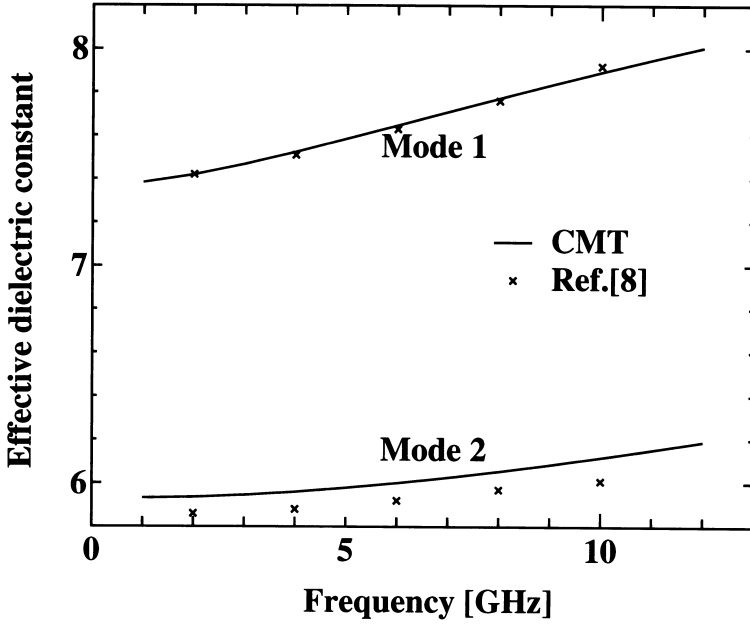


Figure 4. Effective dielectric constants of two nonidentical coupled microstrip lines shown in Fig. 3 with $w_1 = 0.3$ mm, $w_2 = 0.6$ mm, $h_1 = 0.635$ mm, $\epsilon_1 = 9.7$, and $d = 0.4$ mm. CMT refers to the present coupled-mode theory.

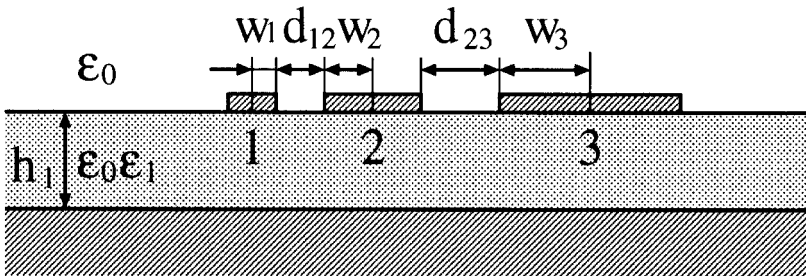


Figure 5. Cross section of three nonidentical coupled microstrip lines.

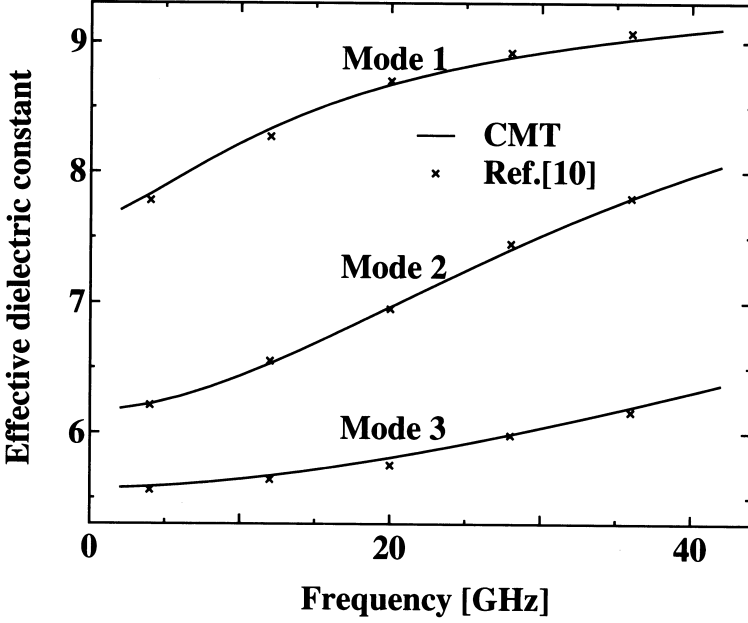
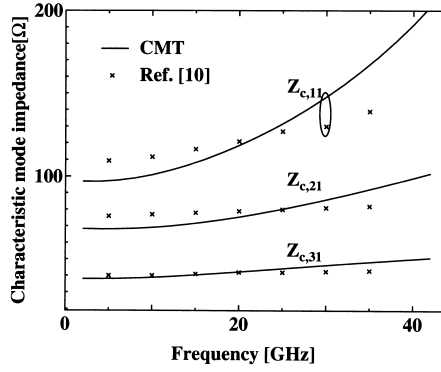
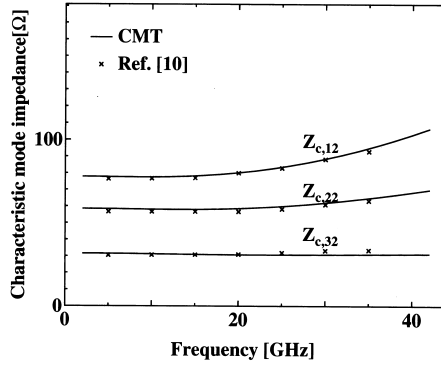


Figure 6. Effective dielectric constants of three nonidentical coupled microstrip lines shown in Fig. 5 with $w_1 = 0.15$ mm, $w_2 = 0.3$ mm, $w_3 = 0.6$ mm, $d_{12} = 0.2$ mm, $d_{23} = 0.4$ mm, $h_1 = 0.635$ mm, $\varepsilon_1 = 9.8$. CMT refers to the present coupled-mode theory.

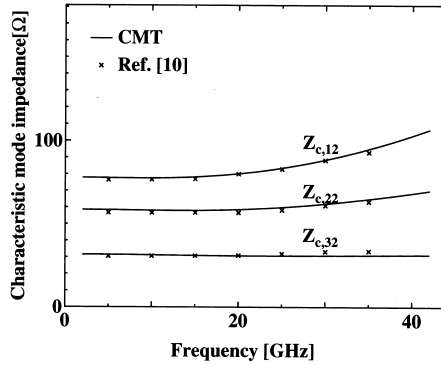
the relative errors for satisfying the relation $Z_{c,11}/Z_{c,21} = Z_{c,12}/Z_{c,22}$ were less than 10^{-2} , whereas the relative errors in the coupled-mode analysis are achieved less than 10^{-4} for the total power and partial power definitions. The characteristic mode impedances at 1 GHz are plotted in Fig. 11 as functions of the separation distance d and compared with those [7] obtained by the direct spectral domain method. Both results are in good agreement. It is seen that $Z_{c,11}$ changes signs very rapidly for values of d around $16\mu\text{m}$. Although this feature has been discussed in [7] from the viewpoint of numerical analysis, we can obtain a clear physical interpretation using the coupled-mode analysis. When two lines are well separated, the solutions of Eq. (7) yield that $a_{11} > 0$, $a_{21} > 0$, $a_{12} < 0$, and $a_{22} > 0$. Then the line currents in modes 1 and 2 flow in the same and opposite directions, respectively, like the even and odd modes of symmetric lines. When the separation



(a) Mode 1



(b) Mode 2



(b) Mode 3

Figure 7. Characteristic mode impedances of three nonidentical coupled microstrip lines. The values of parameters are the same as those in Fig. 6. CMT refers to the present coupled-mode theory.

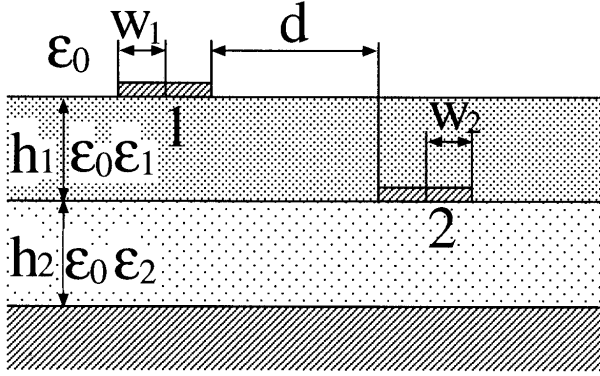


Figure 8. Cross section of two identical coupled microstrip lines in dual planes.

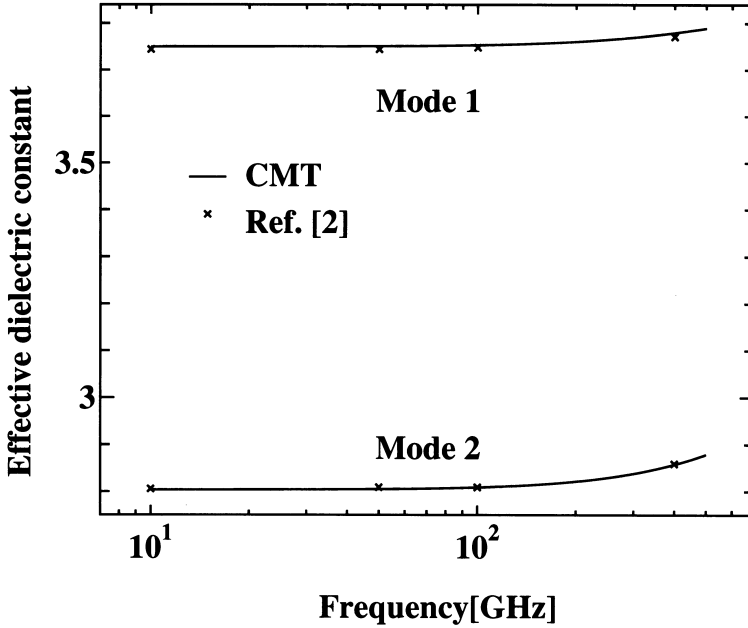


Figure 9. Effective dielectric constants of two nonidentical coupled microstrip lines in dual planes shown in Fig. 8; $w_1 = w_2 = 5\mu\text{m}$, $h_1 = h_2 = 10\mu\text{m}$, $\epsilon_1 = \epsilon_2 = 4.0$, and $d = 30\mu\text{m}$. CMT refers to the present coupled-mode theory.

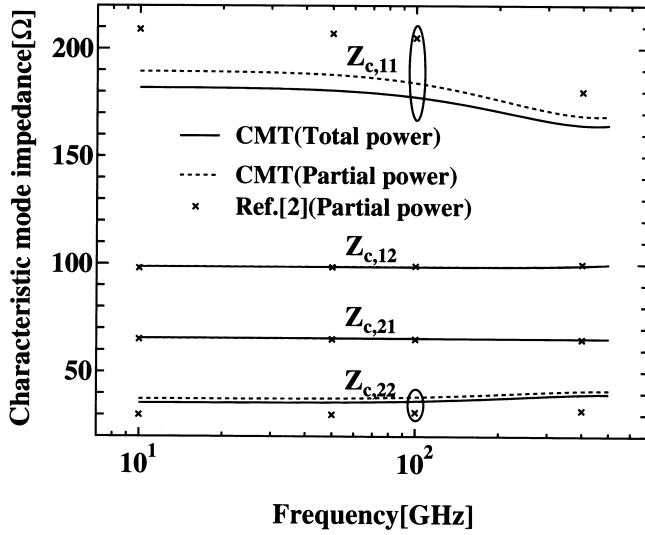


Figure 10. Characteristic mode impedances of two identical coupled microstrip lines in dual planes for $d = 30\mu\text{m}$. The values of other parameters are the same as those in Fig. 9. CMT refers to the present coupled-mode theory.

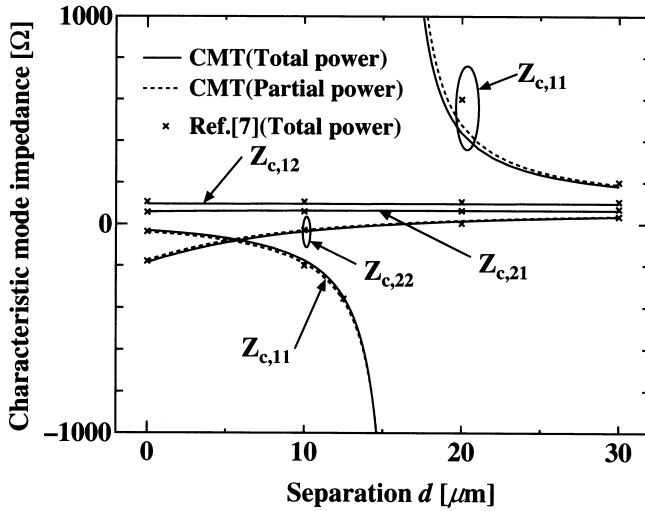


Figure 11. Characteristic mode impedances at 1GHz as functions of separation distance d for two identical coupled microstrip lines in dual planes. The values of other parameters are the same as those in Fig. 9.

distance is decreased, the values of a_{21} , a_{12} , and a_{22} do not show noticeable changes. However the value of a_{11} decreases rapidly, approaches to zero at $d \simeq 16\mu\text{m}$, and change the sign for the further decrease of the separation distance. It follows that the nature of line currents for mode 1 is drastically changed at $d \simeq 16\mu\text{m}$ and mode 1 behaves as a odd mode for $d \gtrsim 16\mu\text{m}$. Referring to Eqs. (20)–(23) or Eqs. (29)–(32), such an anomalous behavior of mode 1 leads to the rapid changes in $Z_{c,11}$ around $d = 16\mu\text{m}$. The line currents of mode 1 is concentrated in line 2 when $d \simeq 16\mu\text{m}$. It is noted that rather than being merely a mathematical approximation, the coupled-mode theory provides good physical insight regarding the coupling effects.

4. CONCLUDING REMARKS

We have presented a coupled-mode theory for line parameters of multilayered coupled microstrip lines. The coupled-mode equations for the amplitudes of line currents have been constituted using the eigenmode fields and currents of each isolated single line. The elements of the coupling matrix were calculated with the solutions of the spectral domain method for the isolated single line. The mode propagation constants and characteristic mode impedances of the coupled lines are easily obtained from the eigenvalues and associated eigenvectors of the coupling matrix. We have presented two expressions for the characteristic mode impedances based on the total power definition and the partial power definition.

The proposed method has been used to analyze the mode propagation constants and characteristic mode impedances for three typical configurations of coupled microstrip lines. The results show a good agreement with those obtained by the direct solution method for the coupled lines.

5. ACKNOWLEDGMENT

This work was supported in part by the Sasakawa Scientific Research Grant from The Japan Science Society and the Grant-in Aid for Scientific Research (B) of The Ministry of Education, Science, Sports and Culture.

REFERENCES

1. Tripathi, V. K., "Asymmetric coupled transmission lines in inhomogeneous medium," *IEEE Trans. Microwave Theory & Tech.*, Vol. MTT-23, 734–739, 1975.
2. Fukuoka, Y., Q. Zhang, D. P. Neikirk, and T. Itoh, "Analysis for multilayer interconnection lines for a high-speed digital integrated circuit," *IEEE Trans. Microwave Theory & Tech.*, Vol. MTT-33, 527–532, 1985.
3. Itoh, T., *Numerical Techniques for Microwave and Millimeter Wave Passive Structures*, John Wiley & Sons, New York, 1989.
4. Yasumoto, K., "Coupled-mode formulation of multilayered and multiconductor transmission lines," *IEEE Trans. Microwave Theory & Tech.*, Vol. MTT-44, 585–590, 1996.
5. Yasumoto, K., and M. Matsunaga, "Coupled-mode analysis of coupled multiple microstrip lines," *IEICE Trans. Electron.*, Vol. E80-C, 340–345, 1997.
6. Weimer, L., and R. H. Jansen, "Reciprocity related definition of strip characteristic impedance for multiconductor hybrid-mode transmission lines," *Microwaves and Opt. Tech. Lett.*, Vol. 1, 22–25, 1988.
7. Carin, L., and K. J. Webb, "Characteristic impedance of multilevel, multiconductor hybrid mode microstrip," *IEEE Trans. Magn.*, Vol. 25, 2947–2949, 1989.
8. Jansen, R. H., "Fast accurate hybrid mode computation of non-symmetrical coupled microstrip characteristics," *Proc. of 7th Eur. Microwave Conf.*, Copenhagen, 135–139, 1977.
9. Bedair, S. S., "Characteristics of some asymmetrical coupled transmission lines", *IEEE Trans. Microwave Theory & Tech.*, Vol. MTT-32, 108–110, 1984.
10. Tripathi, V. K., and H. Lee, "Spectral-domain computation of characteristic impedances and multiport parameters of multiple coupled microstrip lines," *IEEE Trans. Microwave Theory & Tech.*, Vol. MTT-37, 215–221, 1989.
11. Yasumoto, K., M. Matsunaga, and B. S. Rawat, "Coupled-mode theory of terminal characteristic parameters for multilayered and multiconductor lines," *Proc. of 1998 International Conf. on Microwave and Millimeter Wave Technology*, Beijing, 561–564, 1998.